

Review

# Key Issues and Strategies of Aqueous Zinc-Ion Batteries

Yi Liu <sup>1,2</sup>, Huibo Wang <sup>3</sup>, Qingyuan Li <sup>4,\*</sup> , Lingfeng Zhou <sup>4</sup>, Pengjun Zhao <sup>1,\*</sup>  and Rudolf Holze <sup>2,5,6,7</sup> 

- <sup>1</sup> Key Laboratory of Functional Materials and Devices for Special Environments of CAS, Xinjiang Key Laboratory of Electronic Information Materials and Devices, Xinjiang Technical Institute of Physics & Chemistry of CAS, Urumqi 830011, China; liu\_yi@ms.xjb.ac.cn
- <sup>2</sup> Chemnitz University of Technology, D-09107 Chemnitz, Germany; rudolf.holze@chemie.tu-chemnitz.de
- <sup>3</sup> College of Chemical Engineering, Fuzhou University, Fuzhou 350116, China
- <sup>4</sup> Mechanical and Aerospace Engineering Department, Benjamin M. Statler College of Engineering and Mineral Resources, West Virginia University, Morgantown, WV 26506, USA
- <sup>5</sup> Confucius Energy Storage Lab, School of Energy and Environment, Southeast University, Nanjing 210096, China
- <sup>6</sup> Department of Electrochemistry, Institute of Chemistry, Saint Petersburg State University, 7/9 Universitetskaya nab., St. Petersburg 199034, Russia
- <sup>7</sup> State Key Laboratory of Materials-Oriented Chemical Engineering, School of Energy Science and Engineering, Nanjing Tech University, Nanjing 211816, China
- \* Correspondence: qingyuan.li1@mail.wvu.edu (Q.L.); zhaopj@ms.xjb.ac.cn (P.Z.)

**Abstract:** With the rapid growth of the world population and the further industrialization of modern society, the demand for energy continues to rise sharply. Hence, the development of alternative, renewable, and clean energy sources is urgently needed to address the impending energy crisis. Rechargeable aqueous zinc-ion batteries are drawing increased attention and are regarded as the most promising candidates for large-scale energy storage systems. However, some challenges exist for both the anode and cathode, severely restricting the practical application of ZIBs. In this review, we focus on the issues related to the anode (such as dendrites growth, hydrogen evolution, and surface passivation). We discuss the causes of these challenges and summarize the strategies (such as surface engineering, electrolyte modification, and 3D structural skeleton and alloying) to overcome them. Finally, we discuss future opportunities and challenges of ZIBs regarding the Zn anode.

**Keywords:** aqueous zinc ion batteries; Zn anode; surface engineering; electrolyte modification; 3D structural skeleton; alloy strategies



**Citation:** Liu, Y.; Wang, H.; Li, Q.; Zhou, L.; Zhao, P.; Holze, R. Key Issues and Strategies of Aqueous Zinc-Ion Batteries. *Energies* **2023**, *16*, 7443. <https://doi.org/10.3390/en16217443>

Academic Editor: Amir Pakdel

Received: 3 September 2023

Revised: 26 October 2023

Accepted: 1 November 2023

Published: 4 November 2023



**Copyright:** © 2023 by the authors. Licensee MDPI, Basel, Switzerland. This article is an open access article distributed under the terms and conditions of the Creative Commons Attribution (CC BY) license (<https://creativecommons.org/licenses/by/4.0/>).

## 1. Introduction

The research focused on the generation of clean energy has been boosted over the past decades, but the intermittent nature of these renewable resources requires an effective energy storage system (ESS) to store the generated energy. Among the various ESS technologies, rechargeable batteries have been considered the most feasible and reliable, and they already play a prominent role in our lives today. Among them, rechargeable lithium-ion batteries (LIBs) have dominated the application fields of portable devices, electric vehicles, and large-scale energy storage. But, limited lithium resources and the increasing prices of LIBs have aroused great concerns. Therefore, some cheaper rechargeable batteries have received a lot of attention, such as sodium-ion batteries (SIBs), potassium-ion batteries (KIBs), and so on. Despite the significant advancements in SIBs and KIBs, the widespread adoption of organic-based electrolytes, which are toxic, volatile, and flammable, continues to make batteries encounter safety and environmental hurdles. In contrast, aqueous rechargeable batteries offer the advantages of affordability, heightened safety, superior ionic conductivity, and simplified manufacturing. These attributes position aqueous batteries as the most auspicious contender for the forthcoming era of large-scale ESS.

Until now, a variety of aqueous metal-ion batteries, including monovalent ( $\text{Li}^+$ ,  $\text{Na}^+$  and  $\text{K}^+$ ) [1–3], as well as multivalent charge carriers ( $\text{Zn}^{2+}$ ,  $\text{Mg}^{2+}$ ,  $\text{Ca}^{2+}$ , and  $\text{Al}^{3+}$ ) [4–8] have

been investigated. This research trajectory began with Dahn et al.'s initial report in 1994 on the  $\text{VO}_2 \parallel \text{LiMn}_2\text{O}_4$  aqueous battery based on the insertion/extraction mechanism [1]. Compared with other metal anodes, the biggest advantage of metallic zinc is its relative stability and reversible redox reaction in aqueous electrolytes. Table 1 shows the physical and chemical property comparison of monovalent and multivalent metals. According to this comparison and the Pourbaix diagram in Figure 1A,B, we can find that only metallic zinc has the proper redox potential ( $-0.763$  V vs. standard hydrogen electrode (SHE)), which allows Zn to be used directly as an anode in aqueous electrolytes. Combining its high theoretical capacity, low redox potential, nontoxicity, and abundant reserve in the Earth's crust, metallic zinc has been considered the most promising anode material for a large-scale energy storage system. Therefore, Zn-based batteries with mild electrolytes have attracted considerable research interest in the past ten years as a promising aqueous battery.

**Table 1.** Comparison of monovalent and multivalent metals as electrodes. Reproduced with permission [9], Copyright 2019, Elsevier.

Element	Atomic Mass	Standard Potential (V) vs. SHE	Gravimetric Capacity (mAh/g)	Volumetric Capacity (mAh/cm <sup>3</sup> )	Ionic Radius (Å)
Li	6.94	−3.040	3680	2061	0.76
Na	23.00	−2.713	1165	1129	1.02
K	39.1	−2.924	685	610	1.38
Mg	24.31	−2.356	2206	3834	0.72
Ca	40.08	−2.840	1337	2072	1.00
Zn	65.41	−0.763	820	5855	0.75
Al	26.98	−1.676	2980	8046	0.53

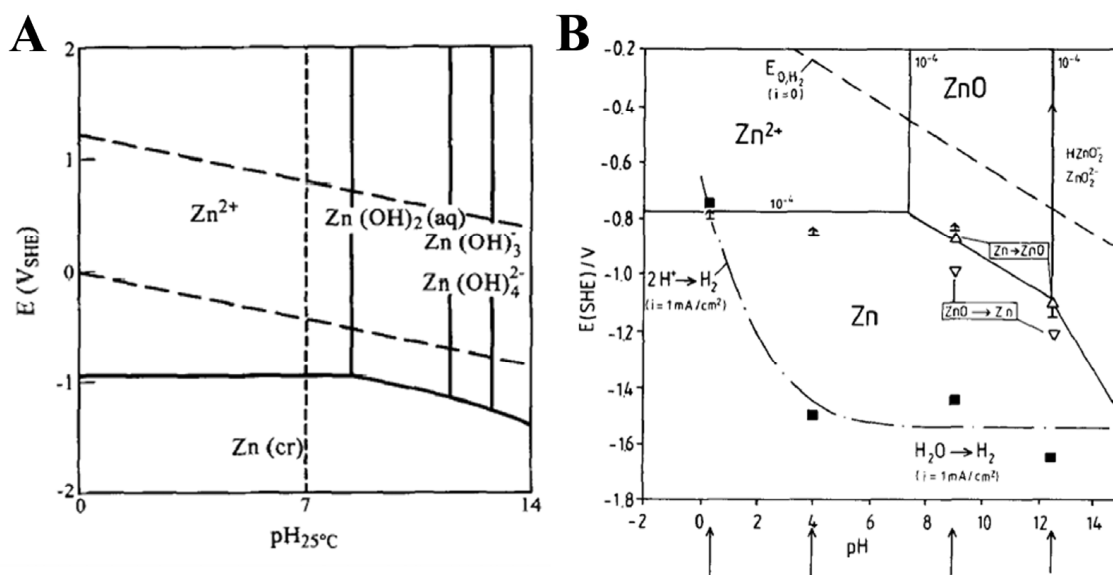


**Figure 1.** (A) Pourbaix diagram of the Zn/H<sub>2</sub>O system. Reproduced with permission [10]. Copyright 1997, Elsevier. (B) Hydrogen evolution reaction overpotential considerations. Reproduced with permission [11]. Copyright 1991, Elsevier.

The energy storage mechanism of the Zn-ion battery is based on the movement of  $\text{Zn}^{2+}$  ions between the cathode and anode, while the electrolyte can be an acidic, neutral, or alkaline solution, depending on the cathode requirement. The operating mechanism of the rechargeable aqueous Zn-ion batteries (ZIBs) is demonstrated in Figure 2. The metal Zn anode undergoes oxidation and reduction ( $\text{Zn} \rightleftharpoons \text{Zn}^{2+} + 2\text{e}^-$ ) during the charge/discharge process. While the reaction mechanism of the cathode is intricate and subject to controversy, it remains a topic of ongoing discussion and is not fully under-

stood. So far, the redox reactions on the cathode side mainly involve three mechanisms:  $\text{Zn}^{2+}$  insertion/extraction [7,12], chemical conversion reaction [13], and  $\text{H}^+/\text{Zn}^{2+}$  insertion/extraction [14,15]. Taking the  $\text{MnO}_2$  cathode as an example, the redox reaction in the  $\text{Zn}^{2+}$  insertion/extraction mechanism is



while the reaction process in the chemical conversion reaction mechanism is as follows:

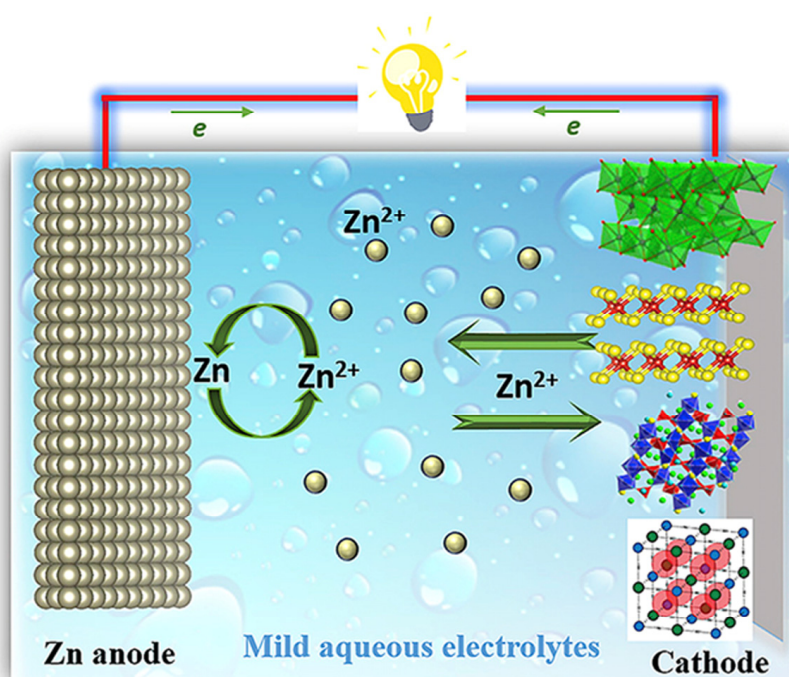
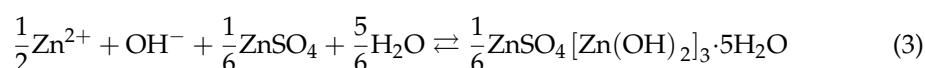


**Figure 2.** Schematic illustration of the aqueous zinc-ion battery in a mildly acidic environment. Reproduced with permission [9]. Copyright 2019, Elsevier.

Thus, the reaction mechanism of highly promising Mn-based cathode materials should be further investigated, and more characterization methods are expected to be adopted to reveal further details of the reaction.

## 2. The Challenges of the Zinc Anode

Even though the research on high-performance ZIBs has achieved great progress, the widespread commercial implementation of metallic zinc anodes in secondary batteries has encountered substantial limitations. Generally, the limitations of ZIB development mainly come from the zinc anode side. The poor rechargeability and low Zn utilization are ascribed to dendrite growth [16–18], hydrogen evolution [19–21], and surface passivation [22–24] occurring on the Zn anodes during the repetitive plating and stripping processes (Figure 3). These factors significantly impede its progress in practical applications in next-generation batteries.

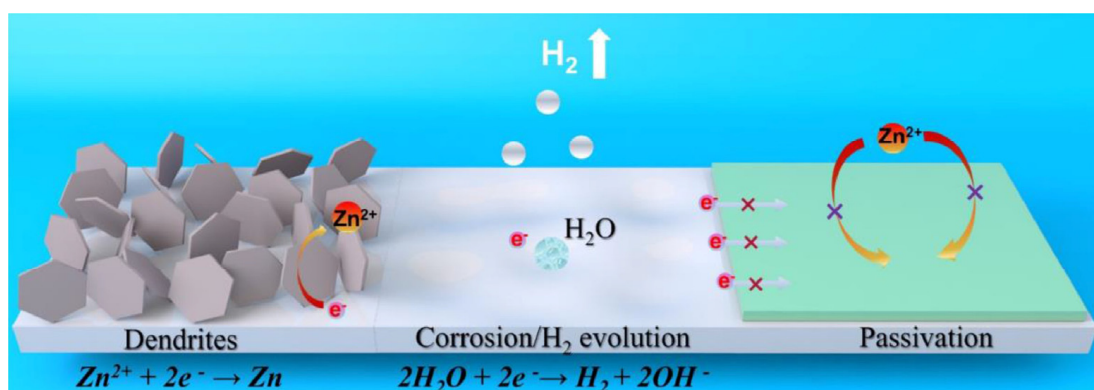


**Figure 3.** Zn anode-related issues in aqueous electrolytes. Reproduced with permission [25]. Copyright 202, Elsevier.

### 2.1. Dendrites and Protrusion

Currently, commercial zinc foils are used as the anode in the ZIBs. However, in practical scenarios, the Zn anodes consistently exhibit uneven and non-uniform surface morphology at the micro- or nanoscale, leading to heterogeneous current distribution and nucleation barriers. During the charge/discharge process, the factors that are responsible for the formation of dendrites are uneven  $Zn^{2+}$  concentration distribution and non-uniform electric field distribution. It is always preferred for the nucleation to occur in locations that have high  $Zn^{2+}$  concentration and a high electric field [24,26]. The formed needle-like protrusion will further promote the growth of zinc dendrites because of the so-called “tip effect”. With repeated charge/discharge cycling, the dendrites will even puncture the separator and give rise to a short circuit during further cycling. In addition, the zinc dendrites will increase the number of Zn anode surface active sites, which further facilitate the corrosion process and hydrogen evolution reaction, leading to low Coulombic efficiency (CE) and speeding up battery deterioration.

### 2.2. Hydrogen Evolution Reaction

In most of the studies, metallic Zn is employed as an anode material in ZIBs directly. However, as a relatively active transition metal, metallic Zn is easily affected by side reactions between Zn electrodes and aqueous electrolytes during the battery operation, which has severely hindered the practical applications of ZIBs. The hydrogen evolution reaction (HER) is the most frequent side reaction during the charge/discharge process in the battery operation. The electrochemical reaction which occurred on the surface of Zn anode is as follows:



The HER not only consumes the fresh electrolyte and Zn anode but also produces  $H_2$  gas, which will lead to the battery swelling. Interestingly, according to ref. [27], a high current density will alleviate the HER during the charge–discharge process. This is because the electrodeposited Zn crystal at high current density has a smaller specific surface area, which is critical for HER activity. As a result, the HER is significantly reduced at high current density.

Furthermore, since most commercial zinc foil is not 100% pure, when the zinc anode is in contact with electrolytes, the impurities present within the anode will combine to create a primary cell with Zn [28]. This micro-cell on the zinc anode will lead to corrosion and  $H_2$  evolution on the surface, which will further push the deterioration of the anode.

### 2.3. Passivation Layer

The surface passivation process is always accompanied by the hydrogen evolution reaction and surface corrosion during the repeated plating/stripping cycling. With the hydrogen evolution, the local pH will be increased dramatically since the  $\text{OH}^-$  concentration increases rapidly [29–31], and the generated  $\text{OH}^-$  will react with  $\text{Zn}^{2+}$  and  $\text{H}_2\text{O}$  to form the passivation layer on the zinc surface. The non-conductive inactive and insoluble byproducts (such as  $\text{ZnO}$  and  $\text{Zn}_4\text{SO}_4(\text{OH})_6 \cdot x\text{H}_2\text{O}$ ) precipitate onto the surface of the zinc anode. This cuts down the reversibility of the plating/stripping process, increases internal resistance, and limits zinc utilization. The accumulation of the non-conductive passivation layer will further reduce the reversibility and enhance the polarization, ultimately leading to the diminished recharging performance of the Zn anode.

## 3. The Strategies of Zinc Anode Protection

The preparation of highly stable and reversible zinc anodes is urgently needed and can provide a high zinc utilization, high CE, and durable cycling life. To solve the problems mentioned in Section 2, tremendous research has been performed, and some effective strategies have been proposed to mitigate the detrimental issues, prolong the lifespan, increase Zn utilization, and improve reversibility. The most promising methods to enhance the lifetime and improve the reversibility of zinc anode are divided into four main categories: surface engineering, electrolyte optimization, structural design, and alloy strategies. For surface engineering, stable and ultrathin artificial protective layers should be well designed to prevent corrosion.

### 3.1. Surface Engineering

Surface engineering appears to be the most direct and effective method to mitigate the degradation of Zn anodes (Figure 4). Two approaches to improve the reversibility of zinc anode via surface engineering are included in this section.

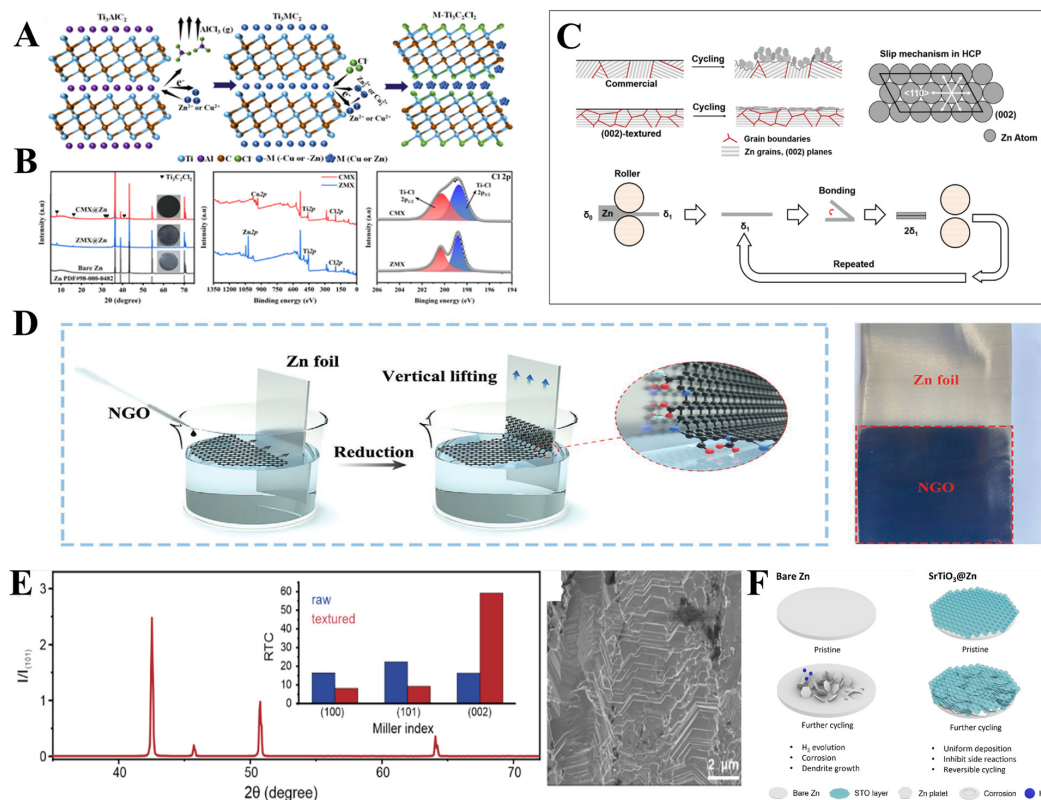


**Figure 4.** (A) Schematic illustration of the preparation of  $\text{Cu}/\text{Ti}_3\text{C}_2\text{Cl}_2$  and  $\text{Zn}/\text{Ti}_3\text{C}_2\text{Cl}_2$  composites. (B) XRD, XPS of bare Zn, ZMX@Zn, CMX@Zn, and Cl 2p spectrum. Reproduced with permission [32].

Copyright 2024, Elsevier. (C) Schematic illustrating how the proposed ARB process can be used to eliminate crystallography heterogeneity of metal electrodes. Reproduced with permission [33]. Copyright 2021, Wiley-VCH. (D) Schematic illustration of fabricating ultrathin graphene layers on the Zn foil. Reproduced with permission [34]. Copyright 2021, Wiley-VCH. (E) XRD spectrum and SEM image of the textured Zn foil. Reproduced with permission [35]. Copyright 2022, Elsevier. (F) Schematic illustration of main advantages of STO@Zn over bare Zn in the mildly acidic aqueous electrolyte. Reproduced with permission [36]. Copyright 2023, Elsevier.

The first is constructing an artificial protecting layer that can work similarly to the SEI in ZIBs. If the commercial zinc foil is directly used as the anode without any modification, it leads to the occurrence of both dendrite growth and side reaction on the surface of the zinc surface. Therefore, an engineered surface layer is constructed to protect the anode from contacting the aqueous electrolyte, effectively curbing dendrite growth and the HER. Hence, building an artificial protection layer on the surface of the zinc anode, whether by an ex situ or in situ method, seems to be essential. Inorganic coating layers, such as  $\text{CaCO}_3$ , [37]  $\text{TiO}_2$ , [38,39] montmorillonite [40,41], carbon materials [42], and other materials [32,43–46] are extensively studied as the protecting layer. The porous nano- $\text{CaCO}_3$  coating layer worked as a buffer layer, which can guide the deposition of Zn during the plating/stripping process [37]. The porous nature of the coating layer can confine the Zn plating reaction beneath the buffer layer, guide uniform electrolyte flux, and control the Zn plating rate, resulting in a uniform and dense Zn deposition layer that can effectively inhibit dendrite formation. In addition, porous nano- $\text{SiO}_2$  and acetylene black were also tested and obtained similar results as the porous nano- $\text{CaCO}_3$ . The  $\text{TiO}_2$  insulating layers are also studied as the protecting layer on the Zn anode surface. By avoiding the direct contact between zinc anode and electrolyte, the undesired hydrogen evolution and corrosion process are significantly suppressed. This protective layer leads to an enhanced electrochemical performance of ZIBs. The protective layer prepared via ALD with (001) facet can effectively prevent the Zn dendrites from vertical growth and stabilize the interface between the electrode and electrolyte; hence, it exhibits a long-term cycle life in the test of plating/stripping performance [38]. The role of crystal orientation of the  $\text{TiO}_2$  protective layer was also studied in the paper, and DFT was used to calculate the interaction between Zn and different facets of  $\text{TiO}_2$ . The calculation results show that the  $\text{TiO}_2$  coating layer with the (001) and (101) facets exposed possesses a relatively low Zn affinity [39]. In addition to the inorganic substances, such as zinc metal anode armor, polymer-based coating layers (such as polyacrylamide, polyamide, poly(vinyl butyral), polyvinylidene fluoride, and others) can serve as barriers to shield against  $\text{H}_2\text{O}/\text{O}_2$  in the electrolyte and exhibit high protective performance in recent studies [47–52]. The polar functional groups contained in the polymers, such as  $\text{C}=\text{O}$  and  $-\text{N}-\text{H}_2$  bonds, can provide abundant adsorption or coordination sites and transfer  $\text{Zn}^{2+}$  to the reaction interface along the polymer chains, which can achieve the regulation of  $\text{Zn}^{2+}$  distribution from the molecular scale through the fast ion pathway. In addition, the polymer layers are water-insoluble and exhibit strong adhesion and excellent flexibility on the Zn surface. With the help of a protective layer, the side reactions with water can be significantly suppressed since the water from the Zn solvation shell was effectively removed during the penetration process, and dendrite growth was remarkably inhibited because of the electrostatic shield effect to avoid the accumulation of  $\text{Zn}^{2+}$ /electrons on local regions.

Even though the inorganic and polymer-protecting layers have their unique features, they also have some shortcomings. The inorganic coating layer has less mechanical flexibility, and the polymer coating layer shows relatively slow kinetics of  $\text{Zn}^{2+}$  transference. Therefore, hybrid coating layers that contain two or more components were also studied [51,53–55], in which the hybrid was designed to use the synergistic effects of different components to enhance the electrochemical performance. For example, Wang et al. [56] fabricate a hybrid coating layer that has carbon black and nano-fibrous cellulose binder; the carbon black can work as the electrically conductive network that can greatly enlarge the

electroactive surface area, and the nano-fibrous cellulose can act as an electrolyte reservoir to facilitate the charge transport. However, the gravimetric and volumetric capacity of complete ZIBs will be inevitably influenced by the introduction of protective layers.

The second method, manipulating the crystallographic orientation of zinc deposition, can effectively get rid of this problem. According to previously published articles [57,58], the (002) plane of metal Zn shows 0~30° alignment to the substrate, while the (100) and (110) planes have a higher angle of 70~90°. Hence, the (002) facet of Zn metal is less likely to facilitate the growth of dendrites when compared with the (100) and (110) planes. In addition, the (002) plane is the closest in hexagonal close-packed (hcp) metal, which has lower thermodynamic free energy than other planes. The decrease in activation energy of the (002) plane enhances the ability of Zn metal to exhibit strong resistance against surface corrosion. Therefore, controlling the growth of deposited zinc during the plating/stripping process is also regarded as one effective method to enhance Zn reversibility [35,59–64]. For example, since graphene possesses the advantage of low lattice mismatch with Zn for the electrodeposition process [65], Zn was preferentially deposited on the graphene substrate with a locked (002) crystallographic orientation during the plating process. The epitaxially electrodeposited Zn exhibits exceptional reversibility over thousands of cycles, whether at moderate or high rates. The (002) enhanced Zn metal can also be prepared via the metal forging method [33,59]. An accumulative roll bonding (ARB) methodology was introduced to prepare the (002) plane preferred Zn foil [33]. The strongly (002)-textured Zn foil was well prepared after a severe plastic deformation process, and the cell cycling test shows that the (002)-textured electrode can still survive for hundreds of charge/discharge cycles even under harsh testing conditions (4 mAh/cm<sup>2</sup> at 40 mA/cm<sup>2</sup>). The Zn (002)-textured surface can also be reached via an acid etching method [66]. After being etched by H<sub>3</sub>PO<sub>4</sub> for 4 min, the ratio of  $I_{(002)}/I_{(100)}$ , which exhibits a (002) plane preference, can reach up to 3.8, and a zinc phosphate protecting layer also forms simultaneously. Owing to the synergistic effect of the enhanced (002) plane and the existence of the Zn<sub>3</sub>(PO<sub>4</sub>)<sub>2</sub> coating layers, the modified electrode exhibits superior electrochemical performance both in the symmetric cell and full battery test. Obviously, the preferred orientation of Zn metal can also be prepared by other methods, and manipulating the crystallographic orientation of zinc deposition during the plating process also can be recognized as an effective way to prolong the lifetime of ZIBs.

### 3.2. Electrolyte Modification

The use of water as an electrolyte solvent enabled the ZIBs to have the advantage of being affordable and nonflammable, with high ionic conductivity and enhanced kinetics. But similar to how every coin has two sides, the water molecules that serve as the solvent will be consumed during the charge/discharge process, and the decomposition of water is the root of the undesired side reaction. In addition, the byproduct and corrosion process will lead to the acceleration of Zn anode deterioration in the following galvanostatic charge/discharge (GCD) process. Due to the tendency of Zn<sup>2+</sup> ions to predominantly exist as hydrated [Zn(H<sub>2</sub>O)<sub>6</sub>]<sup>2+</sup> species in the electrolyte, the aqueous electrolyte exhibits an acidic nature. Additionally, the metal zinc is not thermodynamically stable when exposed to these electrolytes. Therefore, modifying the electrolyte to control the decomposition of water molecules and the behavior of Zn<sup>2+</sup> during the plating/stripping process is also an important strategy to prolong the lifespan of the Zn anode. The most common strategies to improve the batteries' electrochemical performance and suppress the undesired side reaction derived from the electrolyte are mainly categorized into three approaches: highly concentrated electrolyte, hydrogel electrolyte, and functional additives.

#### 3.2.1. Highly Concentrated Electrolyte

The "Water-in-salt" (WiS) electrolyte refers to the electrolyte in which the dissolved salt outnumbers the solvent by both weight and volume; the number of available water molecules that can participate in the ion solvation shell in the WiS electrolyte is far below that in conventional electrolyte [67]. With the limited water content in the electrolyte,

the undesired side reactions triggered by the decomposition of H<sub>2</sub>O that happened on the surface of the zinc anode were highly reduced [68]. In addition, the interaction of the metal ions in the WiS electrolyte replaces the hydrogen bonds with interionic attractions. The high de-solvation energy related to the metal ions with water molecules was significantly reduced, which can facilitate the plating/stripping process [69]. The WiS electrolyte was first proposed in the field of aqueous lithium batteries by Suo et al. in 2015 [70]. With the limited water molecules and improved interionic attractions, the highly concentrated lithium bis(trifluoromethanesulfonyl)imide (LiTFSI)-based WiS electrolyte exhibits a wide electrochemical stable window up to 3.0 V and nearly 100% coulombic efficiency at both low and high charge–discharge rates. When this concept is transferred to ZIBs, super-concentrated electrolytes (such as 1 m Zn(TFSI)<sub>2</sub> with 20 m LiTFSI [71], 1 m Zinc trifluoromethanesulfonate (Zn(CF<sub>3</sub>SO<sub>3</sub>)) with 21 m LiTFSI [72], and 30 m ZnCl<sub>2</sub> [73]) were investigated, and all of these WiS electrolytes exhibit high suppression of dendrite growth and improved zinc anode performance. In addition, the high-concentration electrolyte can also alleviate the dissolution problem of cathode-active materials [68]. But, the introduction of highly concentrated electrolytes will also increase the cost, which will hinder their practical applications.

In addition to the WiS electrolyte, deep eutectic solvents (DESs) also attracted many researchers' attention in the field of energy storage applications due to the merits of low cost, high safety, high ionic conductivity, electrochemical stability, thermal stability, renewability, biodegradable, and easy preparation [74–76]. The radar plots of the properties of DES electrolytes, aqueous electrolytes, and organic liquid electrolytes are demonstrated in Figure 5. Generally, DESs contain large, nonsymmetric ions that have low lattice energy and low melting points, and they are usually prepared by simply combining two or three kinds of inexpensive and safe chemicals [76,77].

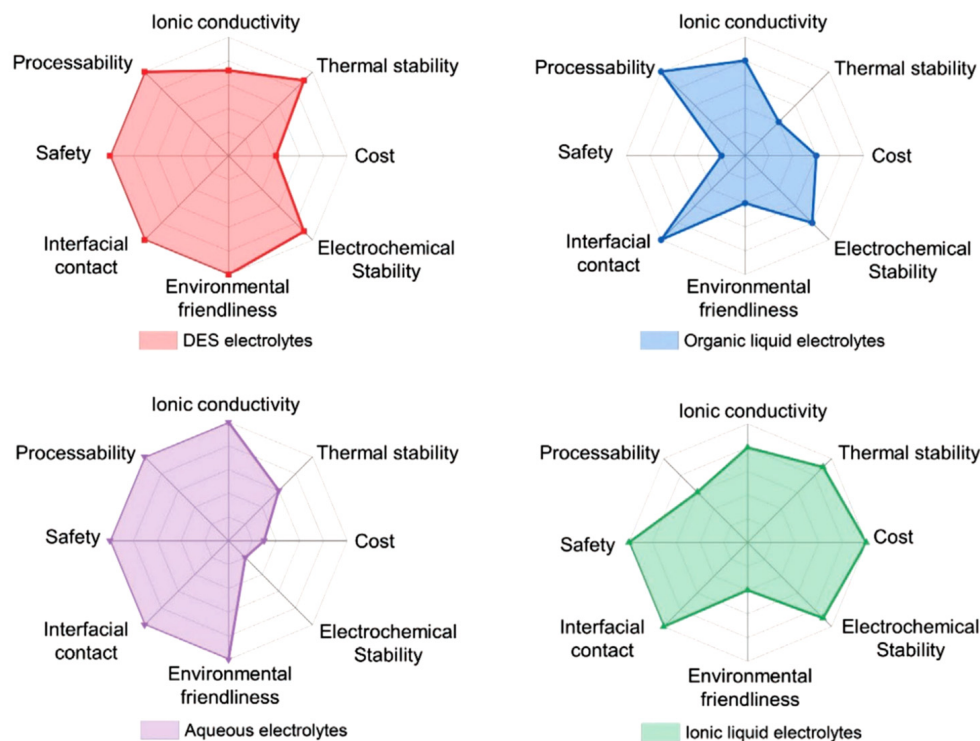


**Figure 5.** Radar plots of the properties of different liquid electrolytes. Reproduced with permission [75]. Copyright 2021, Wiley-VCH.

These DES solutions are receiving more and more attention in ZIBs as electrolytes to improve the full battery performance, and DES electrolytes endow the ZIBs processes with excellent electrochemical performance even at extremely low temperatures. For example,

Shi et al. prepared one kind of DES electrolyte by simply introducing and manipulating the molar ratio of water molecules into a  $\text{ZnCl}_2$ -acetamide electrolyte [78]. The solvation structure of  $\text{Zn}^{2+}$  in the electrolyte was changed, and the de-solvation energy barrier of  $\text{Zn}^{2+}$  was reduced, which can facilitate uniform zinc nucleation during the plating process. With an optimal ratio of  $\text{ZnCl}_2/\text{acetamide}/\text{H}_2\text{O} = 1:3:1$ , the zinc anode shows a highly improved electrochemical performance, with the CE reaching 98% even after 1000 cycles, and the full battery can achieve high-capacity retention of 85.7% even cycled for 10,000 cycles. They also developed one kind of DES electrolyte composed of 3.5 M  $\text{Mg}(\text{ClO}_4)_2$  and 1 M  $\text{Zn}(\text{ClO}_4)_2$ , which can be used at ultra-low temperatures [79]. With the introduction of oxygen-containing ligand-coordinated  $\text{Mg}^{2+}$  ions and hydrogen ligand  $\text{ClO}_4^-$  ions, the hydrogen bonds between the number of water molecules that can drive the formation of ice crystals are significantly decreased and lower the solidifying point to  $-121^\circ\text{C}$ . The DES electrolyte shows high ionic conductivity, low viscosity, and activation even at  $-70^\circ\text{C}$ . The full battery, which was tested at  $-70^\circ\text{C}$ , can still exhibit a high discharge capacity of 101.5 mAh/g at 0.2 A/g and excellent rate performance of 71 mAh/g at 1.2 A/g. Yang et al. reported hydrated eutectic Zn electrolytes by coupling succinonitrile and  $\text{Zn}(\text{ClO}_4)_2 \cdot 6\text{H}_2\text{O}$  with different molar ratios, which also display excellent performance when tested at low temperatures [80]. The participation of succinonitrile in the unique aqueous  $\text{Zn}^{2+}$  solvation shell enables stabilization of the Zn plating/stripping process, and the coulombic efficiency of  $\text{Zn}/\text{Zn}^{2+}$  reversibility can achieve 98.4%. Moreover, all of the water molecules participated in the formation of a eutectic, which delayed the oxidation process and suppressed solvation. When this DES electrolyte was used in the Zn-organic battery, the battery showed an unprecedented cycle ability with a low capacity decay rate (0.004% per cycle over 3500 cycles) and superior low-temperature performance. Since the studies on DESs for ZIBs are still in the very beginning stage, rapid development can be expected because of the merits of DESs [81–83].

### 3.2.2. Hydrogel Electrolytes

Hydrogel electrolytes, which can serve both as electrolytes and separators, have attracted significant attention because of their numerous functional groups, good mechanical properties, and notably constrained active water content in comparison to WiS or DES electrolytes (Figure 6). For this type of electrolyte, zinc salt-containing electrolytes are embedded in the network of polymer chains. The possibility of electrolyte leakage, which always happens in liquid electrolytes, can be highly reduced. These features promote the hydrogel electrolyte to be the most promising candidate for flexible energy storage devices. Gel electrolytes based on polyvinyl alcohol (PVA) [84], xanthan gum [85], and carboxymethyl cellulose (CMC) [86] have been investigated a lot, and all of them have shown an inhibition of dendrite formation and improvement in long-term cycling stability. But, the drawback of zinc salt selectivity and poor mechanical properties restrained their further application. However, the hydrogel electrolytes with cross-linking can effectively solve these problems. Gelatin-based hydrogel electrolyte exhibits much stronger mechanical properties compared with the abovementioned gel electrolytes with the help of hydrogen bonds between -OH, -CO, and -NH<sub>2</sub> functional groups [87]. But, the thermodynamic stability of these gel electrolytes is unsatisfactory. The gel electrolytes with chemical cross-linking possess a more stable network structure, such as polyacrylamide (PAM) [88] and polyacrylic acid (PAA) based gel electrolytes. PAM-based gel electrolytes with 2 M  $\text{ZnSO}_4$  and 0.1 M  $\text{MnSO}_4$  can display a tensile strength of up to 273 kPa and stretch strain higher than 3000% [89].

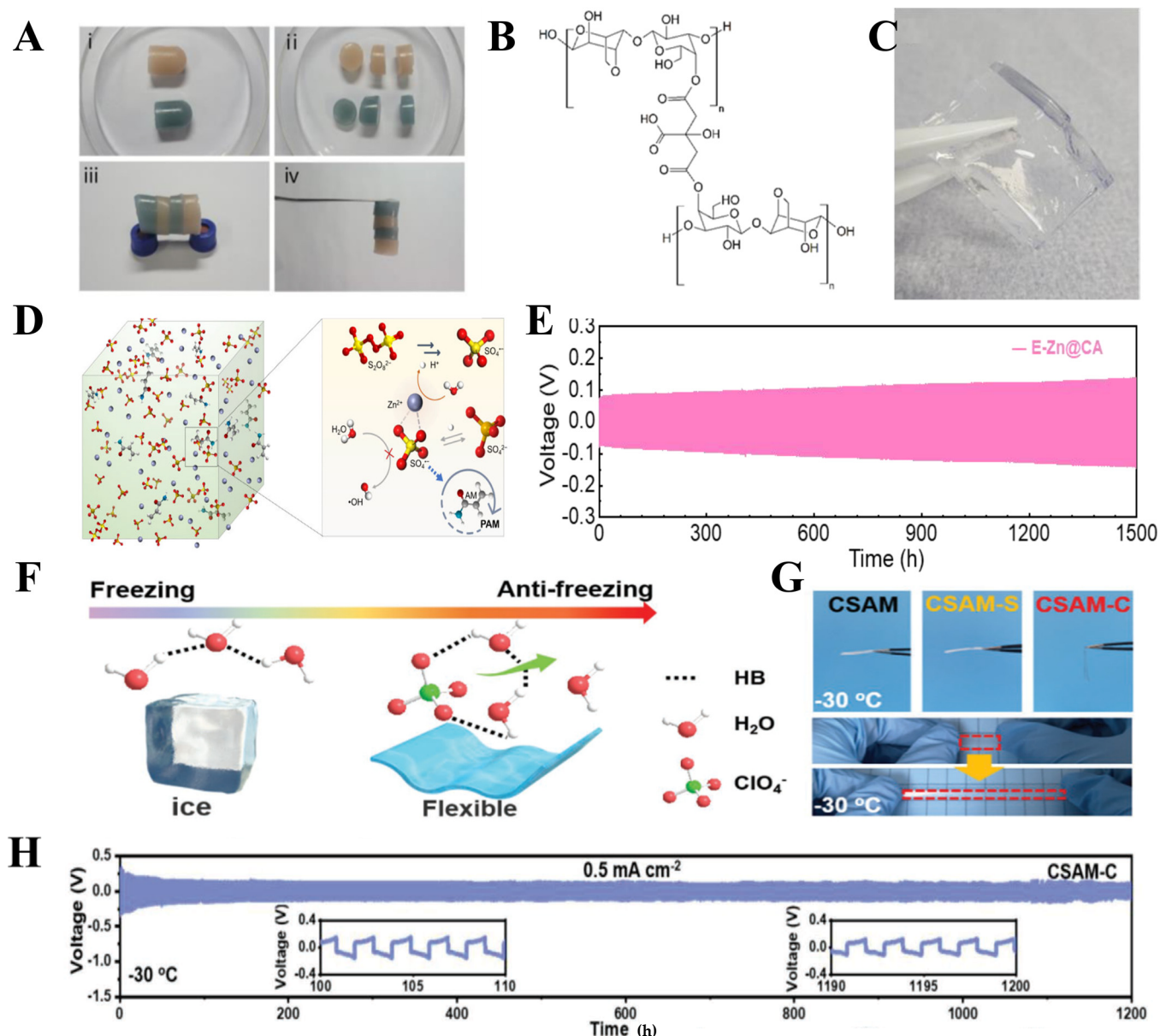


**Figure 6.** (A,D) Self-healing test of MMT-PAM hydrogel and mechanism illustration of the controllable accelerated polymerization strategy. (Pink is the original color of MMT-PAM hydrogel, and the blue-green hydrogel is MMT-PAM hydrogel stained with Prussian blue.) Reproduced with permission [18]. Copyright 2023, Elsevier. (B) Chemical structure of CA protective layer. (C) Digital photograph showing elasticity of CA hydrogel. (E) Long-term galvanostatic cycling performances of symmetrical E-Zn@CA and bare-Zn cells at a current density of  $10 \text{ mA cm}^{-2}$  (areal capacity:  $2 \text{ mAh cm}^{-2}$ ). (B,C,E) Reproduced with permission [20]. Copyright 2022, Elsevier. (F) Schematic illustrations of the hydrogel electrolyte anti-freezing mechanism. (G) Digital images of the CSAM, CSAM-S, and CSAM-C hydrogels after 12 h storage at  $-30 \text{ }^\circ\text{C}$  and the mechanical flexibility demonstration for the CSAM-C hydrogel. (H) Cycling performance of the symmetrical Zn cells with CSAM-C electrolyte under  $0.5 \text{ mA cm}^{-2}$  at  $-30 \text{ }^\circ\text{C}$ . Reproduced with permission [19]. Copyright 2022, Wiley-VCH.

### 3.2.3. Functional Additives

The introduction of functional additives was recognized to be an economical and effective method to improve the Zn reversibility in ZIBs, and it has been proven that even a very small amount of additives can significantly change the morphology of deposited

Zn [90]. The additives can confine the 2D zinc-ion diffusion, regulate the local current distribution, and lower the electrolyte freezing point. According to recent reports, both inorganic ions and organic molecules introduced into electrolytes have shown high efficiency in inhibiting dendrite growth and alleviating the side reaction during the charge/discharge process. The inorganic additives, such as  $\text{InSO}_4$ , [91] Boric acid, [91]  $\text{SnO}_2$ , [91]  $\text{SnCl}_2$ , [92]  $\text{Na}_2\text{SO}_4$ , [15,93], and  $\text{LiCl}$  [94] were used to tune the  $\text{Zn}^{2+}$  deposition process during the plating/stripping cycles (Figure 7). Specifically, the inorganic additives improve the Zn reversibility in the following ways: (1) Manipulating the crystallographic orientation. As discussed in Section 3.1, the (002) plane has lower thermodynamic free energy and moderate angle alignment to the substrate compared with other planes. During the plating/stripping process, the Zn ions can be deposited uniformly, and the battery will show high electrochemical performance. (2) Electrostatic shielding. Due to the low reduction potential of  $\text{Li}^+$  and  $\text{Na}^+$ , they were adsorbed or accumulated much easier than  $\text{Zn}^{2+}$  ions in the local region with high current density. The first adsorbed metal ions will form an electrostatic shielding layer, and this layer will inhibit the tip effect that prevents the  $\text{Zn}^{2+}$  ions from aggregating at these nuclei. As organic additives and many chemicals such as tetrabutylammonium sulfate ( $\text{TBA}_2\text{SO}_4$ ) [95], polyethylene oxide (PEO) [96], polyacrylamide (PAM) [97], and dimethyl sulfoxide (DMSO) [98] were used to prolong the lifetime of ZIBs. Some of these kinds of functional additives can be adsorbed onto the tip of Zn protrusions at the very beginning of the plating process so that the tip effect can be highly suppressed, preventing subsequent deposition of  $\text{Zn}^{2+}$  onto the protrusion. As a result, a consistent and uniform zinc deposition can be facilitated. In addition, some organic additives can decrease the energy barrier of the  $\text{Zn}^{2+}$  de-solvation process, which can accelerate the plating/stripping process and enhance the Zn reversibility. Some of these organic additives possess functional groups that can form a strong bond with a water molecule, which can highly depress the deposition of  $\text{H}_2\text{O}$  and then suppress the HER and side reactions. In addition, some organic additives have special functional groups that can damage the hydrogen bonds when coordinated with a water molecule. With the help of these additives, the freezing point of the electrolyte can be lowered, which can broaden the way to fabricate the aqueous zinc battery at a low temperature.

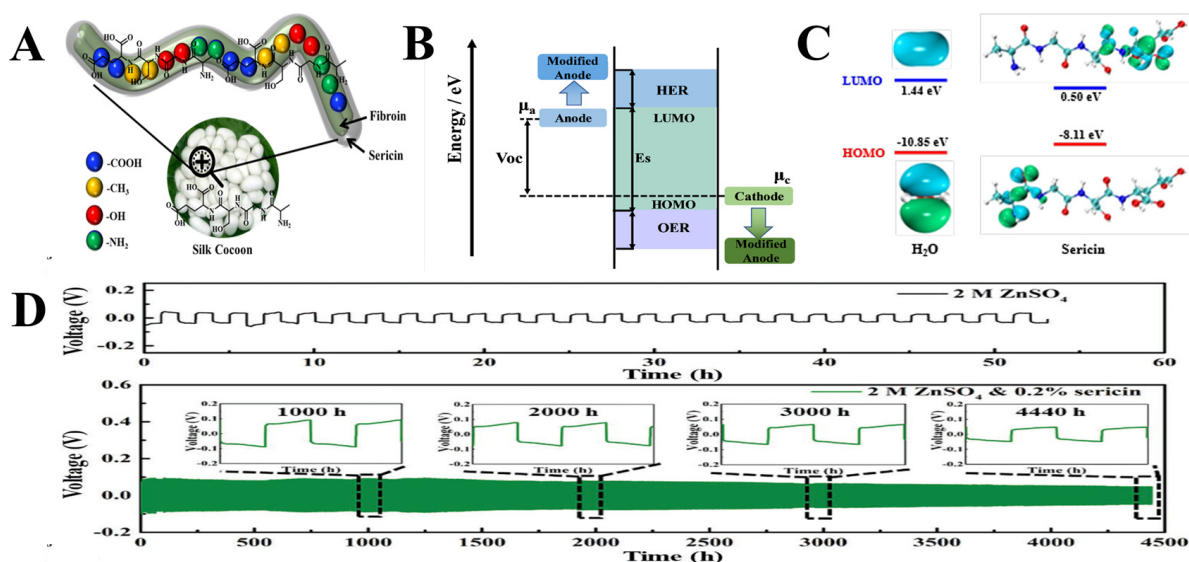
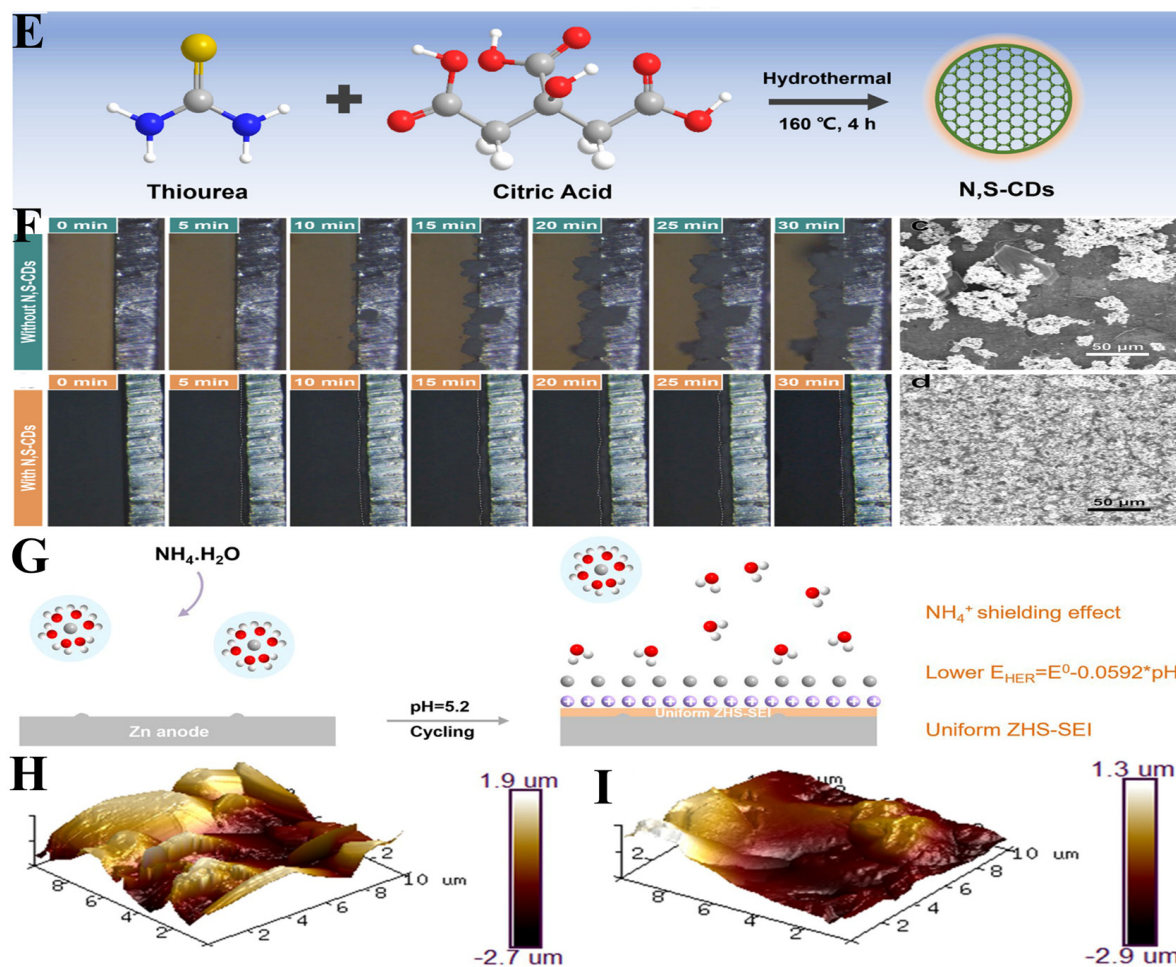


Figure 7. Cont.



**Figure 7.** (A) Schematic of sericin molecules. (B) Relationship between the safe electrochemical window and the energy levels of electrodes/electrolytes according to the frontier molecular orbital theory. (C) Molecular orbital energies of  $\text{H}_2\text{O}$  molecules and sericin molecules. (D) Cycling stability of the Zn symmetrical cells without and with 0.2% sericin additive at  $1.0 \text{ mA cm}^{-2}/1.0 \text{ mAh cm}^{-2}$ . Reproduced with permission [30]. Copyright 2022, Wiley-VCH. (E) Schematic illustration for the preparation process of the N,S-CDs. (F) Observations of the  $\text{Zn}^{2+}$  ion deposition behavior. In situ OM images of the Zn plating process at  $5 \text{ mA cm}^{-2}$  in the electrolyte without and with 0.1% N,S-CDs. Reproduced with permission [99]. Copyright 2023, Royal Society of Chemistry. (G) Schematic illustration of the Zn plating process and in situ observation of Zn plating in the Zn//Zn cell without/with  $\text{NH}_4\text{OH}$  additives. (H,I) AFM image of the Zn anode surface after cycled in electrolyte without/with  $\text{NH}_4\text{OH}$  additive. Reproduced with permission [100]. Copyright 2023, Springer.

### 3.3. Three-Dimensional Structural Skeleton and Alloy Strategies

Building a 3D structural skeleton is another way to effectively restrict dendrite growth and increase the lifetime of the anode [101,102]. Since Zn dendrites are mostly derived from the uneven local current density distribution, the 3D electrode or current collector can provide much more electroactive nucleation sites and homogeneous electrical field distribution when compared with the 2D planar electrode (Figure 8). However, certain conditions need to be met for the design of a 3D electrode or current collector. First, the as-prepared 3D substrate should have the advantages of a highly open architecture, high electronic conductivity, high electrochemical stability, and high corrosion resistance. Then, the 3D structure should also possess high hydrogen evolution overpotential. Based on these rules, metal substrates such as Cu [97] and Ni [103] have been employed in this strategy because they have excellent electronic conductivity and high HER overpotentials. For example, Kang et al. prepared a 3D porous copper-supported Zn anode via a simple

electrodeposition method [104]. The Zn was deposited on the pre-etched porous copper foil; the excellent electrical conductivity and open architecture of the pre-etched copper foil ensure the compact and uniform deposition of Zn during the charge/discharge process, further reducing the polarization and stabilizing the cycling performance. In consideration of the application of ZIBs in the field of portable and wearable devices, the substrates with lightweight, flexible, and elastic conductive carbon-based materials were attempted to be used as current collectors. Therefore, large amounts of carbon-based materials, such as carbon cloth (CC) [105,106], carbon felt (CF) [107], carbon nanotubes (CNTs) [108], and MXene paper [109], were tested as the current collector in recent reports. Most of the carbon-based substrates have hydrophilic groups, which afford the substrate an excellent electrolyte wettability. In addition, the 3D skeletons should have good structural stability to accommodate the zinc metal volume change during the plating/stripping process.

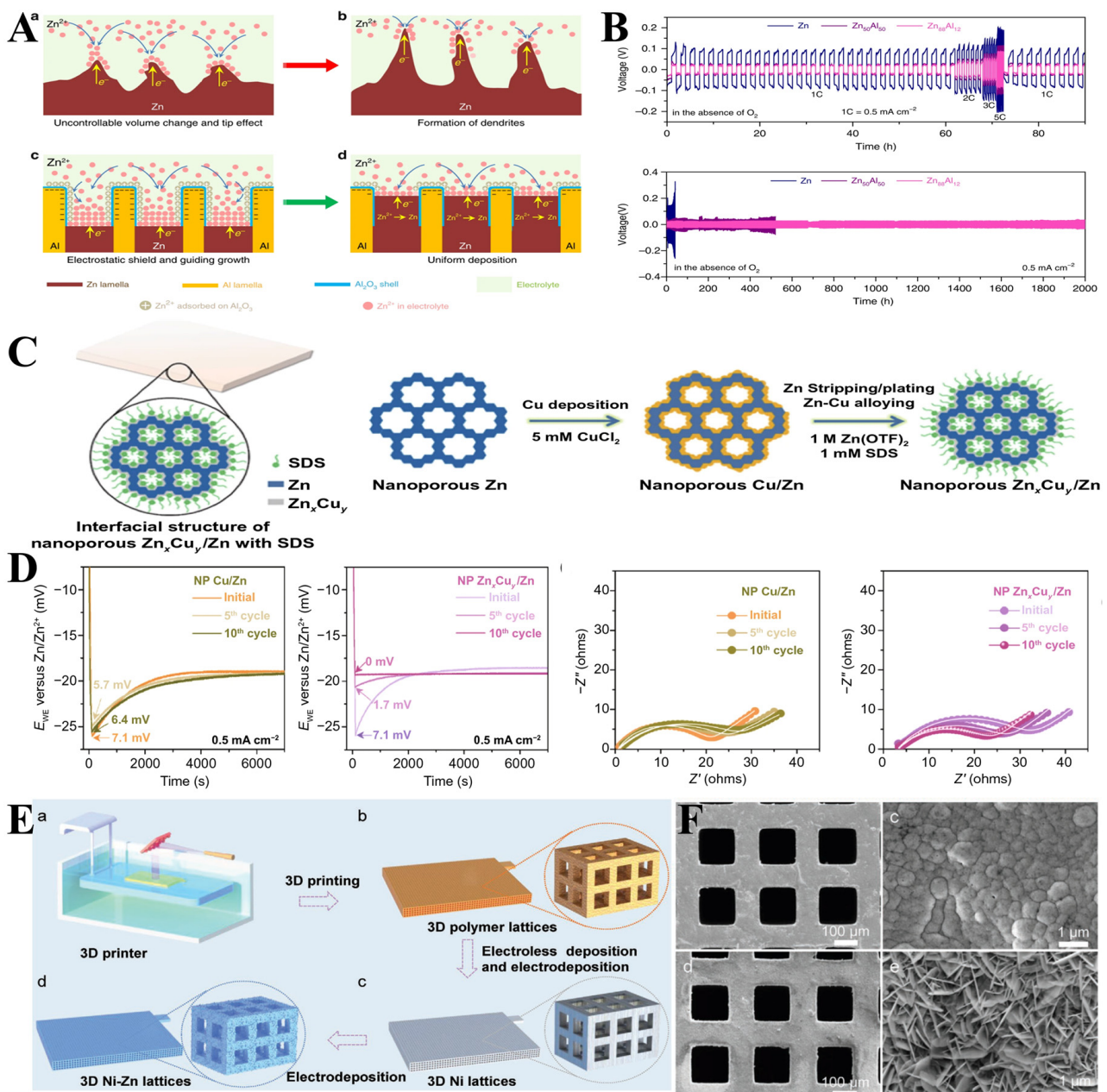
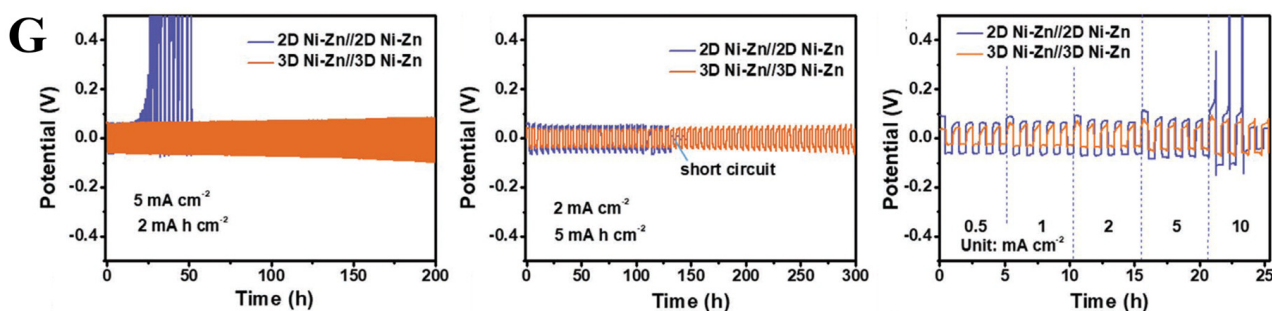


Figure 8. Cont.



**Figure 8.** (A) Schematic illustration of eutectic strategy for dendrite and crack suppression. (B) Rate performance and long-term Zn stripping/plating cycling of symmetric batteries for monometallic Zn, hypoeutectic Zn<sub>50</sub>Al<sub>50</sub>, and eutectic Zn<sub>88</sub>Al<sub>12</sub>. Reproduced with permission [101]. Copyright 2020, Springer. (C). Schematic illustration of nano-porous shell/core Zn<sub>x</sub>Cu<sub>y</sub>/Zn sheets fabrication process. (D) Effect of surface Zn-Cu alloying on Zn deposition. Voltage–time profiles and EIS spectra of galvanostatic Zn deposition on nano-porous Cu/Zn electrode without and with Zn-Cu alloy. Reproduced with permission [16]. Copyright 2022, Springer. (E) Schematic illustration of the procedure for fabricating the 3D Ni–Zn lattices. (F) SEM images with different magnifications of 3D Ni–Zn. (G) Voltage profiles and Rate performance of 2D Ni–Zn symmetric cell and 3D Ni–Zn symmetric cell at different GCD conditions. Reproduced with permission [17]. Copyright 2021, Wiley-VCH.

Alloying zinc with other metals, such as Ga/In [110], Sn [111], Cu [112], P [113], and Al [102], was proposed to be an effective method to improve the lifespan of Zn anode. The introduced foreign metal can work as the 3D current collector during the charge/discharge process; the high electronic conductivity, enlarged electroactive surface, and even electrical field distribution make the alloy anode remarkably effective in suppressing dendrite growth and alleviating the high hydrogen evolution. In addition, the eutectic alloy anodes also have high corrosion resistance, which can highly alleviate the side reaction and corrosion on the electrode. For example, a lamellar-structured Zn/Al eutectic alloy that is composed of alternative zinc and aluminum sheets was reported by Wang et al. [101]. During the plating/stripping process, the Al lamella worked as the 2D skeleton to host the deposited Zn, and the electrostatic shield effect can guide the Zn<sup>2+</sup> to be deposited uniformly; in addition, the aluminum will be oxidized into Al<sub>2</sub>O<sub>3</sub> that can protect the alloy from further dissolution in the electrolyte. Taking advantage of these merits, the eutectic alloy can extend the lifespan of the symmetric cell to 2000 h with a stable overpotential and high coulombic efficiency.

#### 4. Outlook

In this work, the challenges facing zinc metal anodes in mild aqueous ZIBs are discussed, such as zinc dendrites and protrusions, the hydrogen evolution reaction, and the passivation layer existing on the zinc anode surface, and the formation mechanisms are discussed. The strategies to overcome or alleviate these challenges are also provided, for example, the ultra-thin and electrochemically stable protective coating, which should be well designed for high-performance ZIBs, electrolyte modification, and 3D structural skeleton and alloy strategies. Specifically, (1) for the surface engineering, a stable and ultrathin artificial protective layer and surface Zn crystallographic orientation should be well designed to prevent corrosion and the HER and also alleviate dendrite growth; (2) for the electrolyte modification, highly concentrated electrolyte, the hydrogel electrolyte, and functional additives are three promising approaches to enhance ZIBs' electrochemical performance and suppress the undesired side reaction; (3) for the 3D structural skeleton and alloys, the new 3D configuration with more electroactive nucleation sites and homogeneous electrical field distribution should be further investigated. Hence, intensive research with systematic and in-depth comprehension still needs to be performed in this field to elucidate the mechanism of battery failure and to optimize strategies to overcome

the drawbacks. We hope this mini-review will accelerate the development of ZIBs in the laboratory and industry, further investigate their potential commercialization value, and leverage already established manufacturing processes and know-how from the current rechargeable battery industry.

**Author Contributions:** Y.L. conceptualized and wrote the original draft; H.W., Q.L., L.Z., P.Z. and R.H. reviewed and edited the manuscript. All authors have read and agreed to the published version of the manuscript.

**Funding:** This research received no external funding.

**Data Availability Statement:** No new data were created or analyzed in this study. Data sharing is not applicable to this article.

**Acknowledgments:** Yi Liu gratefully acknowledges the support from DAAD.

**Conflicts of Interest:** The authors declare no conflict of interest.

## References

1. Li, W.; Dahn, J.R.; Wainwright, D.S. Rechargeable lithium batteries with aqueous electrolytes. *Science* **1994**, *264*, 1115–1118. [[CrossRef](#)]
2. Suo, L.; Borodin, O.; Wang, Y.; Rong, X.; Sun, W.; Fan, X.; Xu, S.; Schroeder, M.A.; Cresce, A.V.; Wang, F. “Water-in-salt” electrolyte makes aqueous sodium-ion battery safe, green, and long-lasting. *Adv. Energy Mater.* **2017**, *7*, 1701189. [[CrossRef](#)]
3. Su, D.; McDonagh, A.; Qiao, S.Z.; Wang, G. High-capacity aqueous potassium-ion batteries for large-scale energy storage. *Adv. Mater.* **2017**, *29*, 1604007. [[CrossRef](#)] [[PubMed](#)]
4. Chen, L.; Bao, J.; Dong, X.; Truhlar, D.; Wang, Y.; Wang, C.; Xia, Y. Aqueous Mg-ion battery based on polyimide anode and prussian blue cathode. *ACS Energy Lett.* **2017**, *2*, 1115–1121. [[CrossRef](#)]
5. Gheyhani, S.; Liang, Y.; Wu, F.; Jing, Y.; Dong, H.; Rao, K.K.; Chi, X.; Fang, F.; Yao, Y. An aqueous Ca-ion battery. *Adv. Sci.* **2017**, *4*, 1700465. [[CrossRef](#)] [[PubMed](#)]
6. Liu, S.; Pan, G.; Li, G.; Gao, X. Copper hexacyanoferrate nanoparticles as cathode material for aqueous Al-ion batteries. *J. Mater. Chem. A* **2015**, *3*, 959–962. [[CrossRef](#)]
7. Xu, C.; Li, B.; Du, H.; Kang, F. Energetic zinc ion chemistry: The rechargeable zinc ion battery. *Angew. Chem. Int. Ed.* **2012**, *51*, 933–935. [[CrossRef](#)]
8. Liu, Y.; Holze, R. Metal-Ion Batteries. *Encyclopedia* **2022**, *2*, 1611–1623. [[CrossRef](#)]
9. Zeng, X.; Hao, J.; Wang, Z.; Mao, J.; Guo, Z. Recent progress and perspectives on aqueous Zn-based rechargeable batteries with mild aqueous electrolytes. *Energy Storage Mater.* **2019**, *20*, 410–437. [[CrossRef](#)]
10. Beverskog, B.; Puigdomenech, I. Revised pourbaix diagrams for zinc at 25–300 °C. *Corros. Sci.* **1997**, *39*, 107–114. [[CrossRef](#)]
11. Wippermann, K.; Schultze, J.; Kessel, R.; Penninger, J. The inhibition of zinc corrosion by bisaminotriazole and other triazole derivatives. *Corros. Sci.* **1991**, *32*, 205–230. [[CrossRef](#)]
12. Kundu, D.; Adams, B.D.; Duffort, V.; Vajargah, S.H.; Nazar, L.F. A high-capacity and long-life aqueous rechargeable zinc battery using a metal oxide intercalation cathode. *Nat. Energy* **2016**, *1*, 16119. [[CrossRef](#)]
13. Pan, H.; Shao, Y.; Yan, P.; Cheng, Y.; Han, K.S.; Nie, Z.; Wang, C.; Yang, J.; Li, X.; Bhattacharya, P.; et al. Reversible aqueous zinc/manganese oxide energy storage from conversion reactions. *Nat. Energy* **2016**, *1*, 16039. [[CrossRef](#)]
14. Sun, W.; Wang, F.; Hou, S.; Yang, C.; Fan, X.; Ma, Z.; Gao, T.; Han, F.; Hu, R.; Zhu, M. Zn/MnO<sub>2</sub> battery chemistry with H<sup>+</sup> and Zn<sup>2+</sup> coinsertion. *J. Am. Chem. Soc.* **2017**, *139*, 9775–9778. [[CrossRef](#)]
15. Wan, F.; Zhang, L.; Dai, X.; Wang, X.; Niu, Z.; Chen, J. Aqueous rechargeable zinc/sodium vanadate batteries with enhanced performance from simultaneous insertion of dual carriers. *Nat. Commun.* **2018**, *9*, 1656. [[CrossRef](#)] [[PubMed](#)]
16. Meng, H.; Ran, Q.; Dai, T.-Y.; Shi, H.; Zeng, S.-P.; Zhu, Y.-F.; Wen, Z.; Zhang, W.; Lang, X.-Y.; Zheng, W.-T.; et al. Surface-Alloyed Nanoporous Zinc as Reversible and Stable Anodes for High-Performance Aqueous Zinc-Ion Battery. *Nano-Micro Lett.* **2022**, *14*, 128. [[CrossRef](#)]
17. Zhang, G.; Zhang, X.; Liu, H.; Li, J.; Chen, Y.; Duan, H. 3D-Printed Multi-Channel Metal Lattices Enabling Localized Electric-Field Redistribution for Dendrite-Free Aqueous Zn Ion Batteries. *Adv. Energy Mater.* **2021**, *11*, 2003927. [[CrossRef](#)]
18. Ji, S.; Qin, J.; Yang, S.; Shen, P.; Hu, Y.; Yang, K.; Luo, H.; Xu, J. A mechanically durable hybrid hydrogel electrolyte developed by controllable accelerated polymerization mechanism towards reliable aqueous zinc-ion battery. *Energy Storage Mater.* **2023**, *55*, 236–243. [[CrossRef](#)]
19. Huang, S.; Hou, L.; Li, T.; Jiao, Y.; Wu, P. Antifreezing Hydrogel Electrolyte with Ternary Hydrogen Bonding for High-Performance Zinc-Ion Batteries. *Adv. Mater.* **2022**, *34*, 2110140. [[CrossRef](#)]
20. Park, J.-H.; Hyun Park, S.; Joung, D.; Kim, C. Sustainable biopolymeric hydrogel interphase for dendrite-free aqueous zinc-ion batteries. *Chem. Eng. J.* **2022**, *433*, 133532. [[CrossRef](#)]
21. Du, W.; Ang, E.H.; Yang, Y.; Zhang, Y.; Ye, M.; Li, C.C. Challenges in the material and structural design of zinc anode towards high-performance aqueous zinc-ion batteries. *Energy Environ. Sci.* **2020**, *13*, 3330–3360. [[CrossRef](#)]

22. Lu, W.; Zhang, C.; Zhang, H.; Li, X. Anode for Zinc-Based Batteries: Challenges, Strategies, and Prospects. *ACS Energy Lett.* **2021**, *6*, 2765–2785. [[CrossRef](#)]
23. Zheng, J.; Archer, L.A. Controlling electrochemical growth of metallic zinc electrodes: Toward affordable rechargeable energy storage systems. *Sci. Adv.* **2021**, *7*, eabe0219. [[CrossRef](#)] [[PubMed](#)]
24. Zheng, J.; Huang, Z.; Ming, F.; Zeng, Y.; Wei, B.; Jiang, Q.; Qi, Z.; Wang, Z.; Liang, H. Surface and Interface Engineering of Zn Anodes in Aqueous Rechargeable Zn-Ion Batteries. *Small* **2022**, *18*, 2200006. [[CrossRef](#)]
25. He, H.; Qin, H.; Wu, J.; Chen, X.; Huang, R.; Shen, F.; Wu, Z.; Chen, G.; Yin, S.; Liu, J. Engineering interfacial layers to enable Zn metal anodes for aqueous zinc-ion batteries. *Energy Storage Mater.* **2021**, *43*, 317–336. [[CrossRef](#)]
26. Li, Y.; Wu, P.; Zhong, W.; Xie, C.; Xie, Y.; Zhang, Q.; Sun, D.; Tang, Y.; Wang, H.-Y. Progressive nucleation mechanism enables stable zinc stripping-plating behavior. *Energy Environ. Sci.* **2021**, *14*, 5563–5571. [[CrossRef](#)]
27. Yang, Y.; Yang, H.; Zhu, R.; Zhou, H. High reversibility at high current density: The zinc electrodeposition principle behind the “trick”. *Energy Environ. Sci.* **2023**, *16*, 2723–2731. [[CrossRef](#)]
28. Zhang, Y.; Zheng, X.; Wang, N.; Lai, W.-H.; Liu, Y.; Chou, S.-L.; Liu, H.-K.; Dou, S.-X.; Wang, Y.-X. Anode optimization strategies for aqueous zinc-ion batteries. *Chem. Sci.* **2022**, *13*, 14246–14263. [[CrossRef](#)]
29. Zhang, W.; Dai, Y.; Chen, R.; Xu, Z.; Li, J.; Zong, W.; Li, H.; Li, Z.; Zhang, Z.; Zhu, J.; et al. Highly Reversible Zinc Metal Anode in a Dilute Aqueous Electrolyte Enabled by a pH Buffer Additive. *Angew. Chem. Int. Ed.* **2023**, *62*, e202212695. [[CrossRef](#)]
30. Wang, H.; Li, H.; Tang, Y.; Xu, Z.; Wang, K.; Li, Q.; He, B.; Liu, Y.; Ge, M.; Chen, S.; et al. Stabilizing Zn Anode Interface by Simultaneously Manipulating the Thermodynamics of Zn Nucleation and Overpotential of Hydrogen Evolution. *Adv. Funct. Mater.* **2022**, *32*, 2207898. [[CrossRef](#)]
31. Chen, S.; Wang, H.; Zhu, M.; Fan, Y.; Lin, W.; Chan, D.; Lin, W.; Li, P.; Tang, Y.; Zhang, Y. Revitalizing zinc-ion batteries with advanced zinc anode design. *Nanoscale Horiz.* **2023**, *8*, 29–54. [[CrossRef](#)] [[PubMed](#)]
32. Shen, Y.; Liu, Y.; Sun, K.; Gu, T.; Wang, G.; Yang, Y.; Pang, J.; Zheng, Y.; Yang, X.; Chen, L. Zincophilic Ti<sub>3</sub>C<sub>2</sub>Cl<sub>2</sub> MXene and anti-corrosive Cu NPs for synergistically regulated deposition of dendrite-free Zn metal anode. *J. Mater. Sci. Technol.* **2024**, *169*, 137–147. [[CrossRef](#)]
33. Zheng, J.; Deng, Y.; Yin, J.; Tang, T.; Garcia-Mendez, R.; Zhao, Q.; Archer, L.A. Textured Electrodes: Manipulating Built-In Crystallographic Heterogeneity of Metal Electrodes via Severe Plastic Deformation. *Adv. Mater.* **2022**, *34*, 2106867. [[CrossRef](#)]
34. Zhou, J.; Xie, M.; Wu, F.; Mei, Y.; Hao, Y.; Huang, R.; Wei, G.; Liu, A.; Li, L.; Chen, R. Ultrathin Surface Coating of Nitrogen-Doped Graphene Enables Stable Zinc Anodes for Aqueous Zinc-Ion Batteries. *Adv. Mater.* **2021**, *33*, e2101649. [[CrossRef](#)]
35. Liu, Y.; Hu, J.; Lu, Q.; Hantusch, M.; Zhang, H.; Qu, Z.; Tang, H.; Dong, H.; Schmidt, O.G.; Holze, R.; et al. Highly enhanced reversibility of a Zn anode by in-situ texturing. *Energy Storage Mater.* **2022**, *47*, 98–104. [[CrossRef](#)]
36. Ko, J.; So, S.; Kim, M.; Tae Kim, I.; Nam Ahn, Y.; Hur, J. Promoting Zn<sup>2+</sup> migration through polar perovskite dielectric layer on Zn metal anode for the enhanced aqueous Zn-ion batteries. *Chem. Eng. J.* **2023**, *462*, 142308. [[CrossRef](#)]
37. Kang, L.; Cui, M.; Jiang, F.; Gao, Y.; Luo, H.; Liu, J.; Liang, W.; Zhi, C. Nanoporous CaCO<sub>3</sub> coatings enabled uniform Zn stripping/plating for long-life zinc rechargeable aqueous batteries. *Adv. Energy Mater.* **2018**, *8*, 1801090. [[CrossRef](#)]
38. Zhao, K.; Wang, C.; Yu, Y.; Yan, M.; Wei, Q.; He, P.; Dong, Y.; Zhang, Z.; Wang, X.; Mai, L. Ultrathin surface coating enables stabilized zinc metal anode. *Adv. Mater. Interfaces* **2018**, *5*, 1800848. [[CrossRef](#)]
39. Zhang, Q.; Luan, J.; Huang, X.; Wang, Q.; Sun, D.; Tang, Y.; Ji, X.; Wang, H. Revealing the role of crystal orientation of protective layers for stable zinc anode. *Nat. Commun.* **2020**, *11*, 3961. [[CrossRef](#)]
40. Yan, H.; Li, S.; Nan, Y.; Yang, S.; Li, B. Ultrafast zinc-ion-conductor interface toward high-rate and stable zinc metal batteries. *Adv. Energy Mater.* **2021**, *11*, 2100186. [[CrossRef](#)]
41. Hong, L.; Wu, X.; Ma, C.; Huang, W.; Zhou, Y.; Wang, K.-X.; Chen, J.-S. Boosting the Zn-ion transfer kinetics to stabilize the Zn metal interface for high-performance rechargeable Zn-ion batteries. *J. Mater. Chem. A* **2021**, *9*, 16814–16823. [[CrossRef](#)]
42. Zhang, X.; Li, J.; Liu, D.; Liu, M.; Zhou, T.; Qi, K.; Shi, L.; Zhu, Y.; Qian, Y. Ultra-long-life and highly reversible Zn metal anodes enabled by a desolvation and deanionization interface layer. *Energy Environ. Sci.* **2021**, *14*, 3120–3129. [[CrossRef](#)]
43. Liu, P.; Zhang, Z.; Hao, R.; Huang, Y.; Liu, W.; Tan, Y.; Li, P.; Yan, J.; Liu, K. Ultra-highly stable zinc metal anode via 3D-printed g-C<sub>3</sub>N<sub>4</sub> modulating interface for long life energy storage systems. *Chem. Eng. J.* **2021**, *403*, 126425. [[CrossRef](#)]
44. Han, J.; Euchner, H.; Kuenzel, M.; Hosseini, S.M.; Groß, A.; Varzi, A.; Passerini, S. A thin and uniform fluoride-based artificial interphase for the zinc metal anode enabling reversible Zn/MnO<sub>2</sub> batteries. *ACS Energy Lett.* **2021**, *6*, 3063–3071. [[CrossRef](#)]
45. Wu, J.; Yuan, C.; Li, T.; Yuan, Z.; Zhang, H.; Li, X. Dendrite-free zinc-based battery with high areal capacity via the region-induced deposition effect of turing membrane. *J. Am. Chem. Soc.* **2021**, *143*, 13135–13144. [[CrossRef](#)]
46. Lu, Q.; Liu, C.; Du, Y.; Wang, X.; Ding, L.; Omar, A.; Mikhailova, D. Uniform Zn Deposition Achieved by Ag Coating for Improved Aqueous Zinc-Ion Batteries. *ACS Appl. Mater. Interfaces* **2021**, *13*, 16869–16875. [[CrossRef](#)] [[PubMed](#)]
47. Cao, L.; Li, D.; Deng, T.; Li, Q.; Wang, C. Hydrophobic organic-electrolyte-protected zinc anodes for aqueous zinc batteries. *Angew. Chem. Int. Ed.* **2020**, *59*, 19292–19296. [[CrossRef](#)] [[PubMed](#)]
48. Chen, P.; Yuan, X.; Xia, Y.; Zhang, Y.; Fu, L.; Liu, L.; Yu, N.; Huang, Q.; Wang, B.; Hu, X.; et al. An artificial polyacrylonitrile coating layer confining zinc dendrite growth for highly reversible aqueous zinc-based batteries. *Adv. Sci.* **2021**, *8*, e2100309. [[CrossRef](#)] [[PubMed](#)]
49. Zhao, Z.; Zhao, J.; Hu, Z.; Li, J.; Li, J.; Zhang, Y.; Wang, C.; Cui, G. Long-life and deeply rechargeable aqueous Zn anodes enabled by a multifunctional brightener-inspired interphase. *Energy Environ. Sci.* **2019**, *12*, 1938–1949. [[CrossRef](#)]

50. Park, S.H.; Byeon, S.Y.; Park, J.-H.; Kim, C. Insight into the critical role of surface hydrophilicity for dendrite-free zinc metal anodes. *ACS Energy Lett.* **2021**, *6*, 3078–3085. [[CrossRef](#)]
51. Zhao, R.; Yang, Y.; Liu, G.; Zhu, R.; Huang, J.; Chen, Z.; Gao, Z.; Chen, X.; Qie, L. Redirected Zn electrodeposition by an anti-corrosion elastic constraint for highly reversible Zn anodes. *Adv. Funct. Mater.* **2020**, *31*, 2001867. [[CrossRef](#)]
52. Hao, J.; Li, X.; Zhang, S.; Yang, F.; Zeng, X.; Zhang, S.; Bo, G.; Wang, C.; Guo, Z. Designing dendrite-free zinc anodes for advanced aqueous zinc batteries. *Adv. Funct. Mater.* **2020**, *30*, 2001263. [[CrossRef](#)]
53. Zhou, S.; Wang, Y.P.; Lu, H.T.; Zhang, Y.F.; Fu, C.Y.; Usman, I.; Liu, Z.X.; Feng, M.Y.; Fang, G.Z.; Cao, X.X.; et al. Anti-corrosive and Zn-ion-regulating composite interlayer enabling long-life Zn metal anodes. *Adv. Funct. Mater.* **2021**, *31*, 2104361. [[CrossRef](#)]
54. Chu, Y.; Zhang, S.; Wu, S.; Hu, Z.; Cui, G.; Luo, J. In situ built interphase with high interface energy and fast kinetics for high performance Zn metal anodes. *Energy Environ. Sci.* **2021**, *14*, 3609–3620. [[CrossRef](#)]
55. Li, D.; Cao, L.; Deng, T.; Liu, S.; Wang, C. Design of a solid electrolyte interphase for aqueous Zn batteries. *Angew. Chem. Int. Ed.* **2021**, *60*, 13035–13041. [[CrossRef](#)] [[PubMed](#)]
56. Wang, A.; Zhou, W.; Huang, A.; Chen, M.; Chen, J.; Tian, Q.; Xu, J. Modifying the Zn anode with carbon black coating and nanofibrillated cellulose binder: A strategy to realize dendrite-free Zn-MnO<sub>2</sub> batteries. *J. Colloid Interface Sci.* **2020**, *577*, 256–264. [[CrossRef](#)]
57. Sawada, Y. Transition of growth form from dendrite to aggregate. *Phys. A Stat. Mech. Its Appl.* **1986**, *140*, 134–141. [[CrossRef](#)]
58. Mackinnon, D.J.; Brannen, J.M.; Fenn, P.L. Characterization of impurity effects in zinc electrowinning from industrial acid sulphate electrolyte. *J. Appl. Electrochem.* **1987**, *17*, 1129–1143. [[CrossRef](#)]
59. Zhou, M.; Guo, S.; Li, J.; Luo, X.; Liu, Z.; Zhang, T.; Cao, X.; Long, M.; Lu, B.; Pan, A.; et al. Surface-preferred crystal plane for a stable and reversible zinc anode. *Adv. Mater.* **2021**, *33*, 2100187. [[CrossRef](#)]
60. Zheng, J.; Bock, D.C.; Tang, T.; Zhao, Q.; Yin, J.; Tallman, K.R.; Wheeler, G.; Liu, X.; Deng, Y.; Jin, S.; et al. Regulating electrodeposition morphology in high-capacity aluminium and zinc battery anodes using interfacial metal–substrate bonding. *Nat. Energy* **2021**, *6*, 398–406. [[CrossRef](#)]
61. Li, S.; Fu, J.; Miao, G.; Wang, S.; Zhao, W.; Wu, Z.; Zhang, Y.; Yang, X. Toward planar and dendrite-free Zn electrodepositions by regulating Sn-crystal textured surface. *Adv. Mater.* **2021**, *33*, 2008424. [[CrossRef](#)]
62. Cao, J.; Zhang, D.; Gu, C.; Wang, X.; Wang, S.; Zhang, X.; Qin, J.; Wu, Z.S. Manipulating crystallographic orientation of zinc deposition for dendrite-free zinc ion batteries. *Adv. Energy Mater.* **2021**, *11*, 2101299. [[CrossRef](#)]
63. Zheng, J.; Yin, J.; Zhang, D.; Li, G.; Bock, D.C.; Tang, T.; Zhao, Q.; Liu, X.; Warren, A.; Deng, Y.; et al. Spontaneous and field-induced crystallographic reorientation of metal electrodeposits at battery anodes. *Sci. Adv.* **2020**, *6*, eabb1122. [[CrossRef](#)] [[PubMed](#)]
64. Yuan, D.; Zhao, J.; Ren, H.; Chen, Y.; Chua, R.; Jie, E.T.J.; Cai, Y.; Edison, E.; Manalastas, W., Jr.; Wong, M.W.; et al. Anion texturing towards dendrite-free Zn anode for aqueous rechargeable batteries. *Angew. Chem. Int. Ed.* **2021**, *60*, 7213–7219. [[CrossRef](#)]
65. Zheng, J.; Zhao, Q.; Tang, T.; Yin, J.; Quilty, C.D.; Renderos, G.D.; Liu, X.; Deng, Y.; Wang, L.; Bock, D.C.; et al. Reversible epitaxial electrodeposition of metals in battery anodes. *Science* **2019**, *366*, 645–648. [[CrossRef](#)]
66. Wang, X.; Meng, J.; Lin, X.; Yang, Y.; Zhou, S.; Wang, Y.; Pan, A. Stable zinc metal anodes with textured crystal faces and functional zinc compound coatings. *Adv. Funct. Mater.* **2021**, *31*, 2106114. [[CrossRef](#)]
67. Wang, Y.; Meng, X.; Sun, J.; Liu, Y.; Hou, L. Recent progress in “water-in-salt” electrolytes toward non-lithium based rechargeable batteries. *Front. Chem.* **2020**, *8*, 595. [[CrossRef](#)]
68. Droguet, L.; Grimaud, A.; Fontaine, O.; Tarascon, J.-M. Water-in-Salt electrolyte (WiSE) for aqueous batteries: A long way to practicality. *Adv. Energy Mater.* **2020**, *10*, 2002440. [[CrossRef](#)]
69. Azov, V.A.; Egorova, K.S.; Seitkalieva, M.M.; Kashin, A.S.; Ananikov, V.P. “Solvent-in-salt” systems for design of new materials in chemistry, biology and energy research. *Chem. Soc. Rev.* **2018**, *47*, 1250–1284. [[CrossRef](#)]
70. Suo, L.; Borodin, O.; Gao, T.; Olguin, M.; Ho, J.; Fan, X.; Luo, C.; Wang, C.; Xu, K. “Water-in-salt” electrolyte enables high-voltage aqueous lithium-ion chemistries. *Science* **2015**, *350*, 938–943. [[CrossRef](#)] [[PubMed](#)]
71. Wang, F.; Borodin, O.; Gao, T.; Fan, X.; Sun, W.; Han, F.; Faraone, A.; Dura, J.A.; Xu, K.; Wang, C. Highly reversible zinc metal anode for aqueous batteries. *Nat. Mater.* **2018**, *17*, 543–549. [[CrossRef](#)]
72. Hu, P.; Yan, M.; Zhu, T.; Wang, X.; Wei, X.; Li, J.; Zhou, L.; Li, Z.; Chen, L.; Mai, L. Zn/V<sub>2</sub>O<sub>5</sub> aqueous hybrid-ion battery with high voltage platform and long cycle life. *ACS Appl. Mater. Interfaces* **2017**, *9*, 42717–42722. [[CrossRef](#)] [[PubMed](#)]
73. Zhang, C.; Holoubek, J.; Wu, X.; Daniyar, A.; Zhu, L.; Chen, C.; Leonard, D.P.; Rodríguez-Pérez, I.A.; Jiang, J.-X.; Fang, C.; et al. A ZnCl<sub>2</sub> water-in-salt electrolyte for a reversible Zn metal anode. *Chem. Commun.* **2018**, *54*, 14097–14099. [[CrossRef](#)] [[PubMed](#)]
74. Kohli, R. Chapter 16—Applications of Ionic Liquids in Removal of Surface Contaminants. In *Developments in Surface Contamination and Cleaning: Applications of Cleaning Techniques*; Kohli, R., Mittal, K.L., Eds.; Elsevier: Amsterdam, The Netherlands, 2019; pp. 619–680.
75. Wu, J.; Liang, Q.; Yu, X.; Lü, Q.-F.; Ma, L.; Qin, X.; Chen, G.; Li, B. Deep eutectic solvents for boosting electrochemical energy storage and conversion: A review and perspective. *Adv. Funct. Mater.* **2021**, *31*, 2011102. [[CrossRef](#)]
76. Smith, E.L.; Abbott, A.P.; Ryder, K.S. Deep eutectic solvents (DESs) and their applications. *Chem. Rev.* **2014**, *114*, 11060–11082. [[CrossRef](#)] [[PubMed](#)]
77. Hansen, B.B.; Spittle, S.; Chen, B.; Poe, D.; Zhang, Y.; Klein, J.M.; Horton, A.; Adhikari, L.; Zelovich, T.; Doherty, B.W.; et al. Deep eutectic solvents: A review of fundamentals and applications. *Chem. Rev.* **2021**, *121*, 1232–1285. [[CrossRef](#)]

78. Shi, J.; Sun, T.; Bao, J.; Zheng, S.; Du, H.; Li, L.; Yuan, X.; Ma, T.; Tao, Z. “Water-in-deep eutectic solvent” electrolytes for high-performance aqueous Zn-ion batteries. *Adv. Funct. Mater.* **2021**, *31*, 2102035. [[CrossRef](#)]
79. Sun, T.; Zheng, S.; Du, H.; Tao, Z. Synergistic effect of cation and anion for low-temperature aqueous zinc-ion battery. *Nano-Micro Lett.* **2021**, *13*, 204. [[CrossRef](#)]
80. Yang, W.; Du, X.; Zhao, J.; Chen, Z.; Li, J.; Xie, J.; Zhang, Y.; Cui, Z.; Kong, Q.; Zhao, Z.; et al. Hydrated eutectic electrolytes with ligand-oriented solvation shells for long-cycling Zinc-organic batteries. *Joule* **2020**, *4*, 1557–1574. [[CrossRef](#)]
81. Ghareh Bagh, F.S.; Shahbaz, K.; Mjalli, F.S.; Hashim, M.A.; AlNashef, I.M. Zinc (II) chloride-based deep eutectic solvents for application as electrolytes: Preparation and characterization. *J. Mol. Liq.* **2015**, *204*, 76–83. [[CrossRef](#)]
82. Zhao, J.; Zhang, J.; Yang, W.; Chen, B.; Zhao, Z.; Qiu, H.; Dong, S.; Zhou, X.; Cui, G.; Chen, L. “Water-in-deep eutectic solvent” electrolytes enable zinc metal anodes for rechargeable aqueous batteries. *Nano Energy* **2019**, *57*, 625–634. [[CrossRef](#)]
83. Qiu, H.; Du, X.; Zhao, J.; Wang, Y.; Ju, J.; Chen, Z.; Hu, Z.; Yan, D.; Zhou, X.; Cui, G. Zinc anode-compatible in-situ solid electrolyte interphase via cation solvation modulation. *Nat. Commun.* **2019**, *10*, 5374. [[CrossRef](#)]
84. Zeng, Y.; Zhang, X.; Meng, Y.; Yu, M.; Yi, J.; Wu, Y.; Lu, X.; Tong, Y. Achieving ultrahigh energy density and long durability in a flexible rechargeable quasi-solid-state Zn–MnO<sub>2</sub> battery. *Adv. Mater.* **2017**, *29*, 1700274. [[CrossRef](#)]
85. Zhang, S.; Yu, N.; Zeng, S.; Zhou, S.; Chen, M.; Di, J.; Li, Q. An adaptive and stable bio-electrolyte for rechargeable Zn-ion batteries. *J. Mater. Chem. A* **2018**, *6*, 12237–12243. [[CrossRef](#)]
86. Zhang, Q.; Li, C.; Li, Q.; Pan, Z.; Sun, J.; Zhou, Z.; He, B.; Man, P.; Xie, L.; Kang, L. Flexible and high-voltage coaxial-fiber aqueous rechargeable zinc-ion battery. *Nano Lett.* **2019**, *19*, 4035–4042. [[CrossRef](#)]
87. McEvoy, H.; Ross-Murphy, S.; Clark, A. Large deformation and ultimate properties of biopolymer gels: 1. Single biopolymer component systems. *Polymer* **1985**, *26*, 1483–1492. [[CrossRef](#)]
88. Ma, L.; Chen, S.; Wang, D.; Yang, Q.; Mo, F.; Liang, G.; Li, N.; Zhang, H.; Zapfen, J.A.; Zhi, C. Super-stretchable Zinc-Air batteries based on an alkaline-tolerant dual-network hydrogel electrolyte. *Adv. Energy Mater.* **2019**, *9*, 1803046. [[CrossRef](#)]
89. Li, H.; Liu, Z.; Liang, G.; Huang, Y.; Huang, Y.; Zhu, M.; Pei, Z.; Xue, Q.; Tang, Z.; Wang, Y.; et al. Waterproof and tailorable elastic rechargeable yarn zinc ion batteries by a cross-linked polyacrylamide electrolyte. *ACS Nano* **2018**, *12*, 3140–3148. [[CrossRef](#)] [[PubMed](#)]
90. Li, C.; Xie, X.; Liang, S.; Zhou, J. Issues and future perspective on zinc metal anode for rechargeable aqueous zinc-ion batteries. *Energy Environ. Mater.* **2020**, *3*, 146–159. [[CrossRef](#)]
91. Sun, K.E.K.; Hoang, T.K.A.; Doan, T.N.L.; Yu, Y.; Chen, P. Highly sustainable zinc anodes for a rechargeable hybrid aqueous battery. *Chemistry* **2018**, *24*, 1667–1673. [[CrossRef](#)]
92. Trudgeon, D.P.; Qiu, K.; Li, X.; Mallick, T.; Taiwo, O.O.; Chakrabarti, B.; Yufit, V.; Brandon, N.P.; Crevillen-Garcia, D.; Shah, A. Screening of effective electrolyte additives for zinc-based redox flow battery systems. *J. Power Sources* **2019**, *412*, 44–54. [[CrossRef](#)]
93. Xu, Y.; Zhu, J.; Feng, J.; Wang, Y.; Wu, X.; Ma, P.; Zhang, X.; Wang, G.; Yan, X. A rechargeable aqueous zinc/sodium manganese oxides battery with robust performance enabled by Na<sub>2</sub>SO<sub>4</sub> electrolyte additive. *Energy Storage Mater.* **2021**, *38*, 299–308. [[CrossRef](#)]
94. Guo, X.; Zhang, Z.; Li, J.; Luo, N.; Chai, G.-L.; Miller, T.S.; Lai, F.; Shearing, P.; Brett, D.J.L.; Han, D.; et al. Alleviation of dendrite formation on zinc anodes via electrolyte additives. *ACS Energy Lett.* **2021**, *6*, 395–403. [[CrossRef](#)]
95. Bayaguud, A.; Luo, X.; Fu, Y.; Zhu, C. Cationic surfactant-type electrolyte additive enables three-dimensional dendrite-free zinc anode for stable zinc-ion batteries. *ACS Energy Lett.* **2020**, *5*, 3012–3020. [[CrossRef](#)]
96. Jin, Y.; Han, K.S.; Shao, Y.; Sushko, M.L.; Xiao, J.; Pan, H.; Liu, J. Stabilizing zinc anode reactions by polyethylene oxide polymer in mild aqueous electrolytes. *Adv. Funct. Mater.* **2020**, *30*, 2003932. [[CrossRef](#)]
97. Zhang, Q.; Luan, J.; Fu, L.; Wu, S.; Tang, Y.; Ji, X.; Wang, H. The three-dimensional dendrite-free zinc anode on a copper mesh with a zinc-oriented polyacrylamide electrolyte additive. *Angew. Chem. Int. Ed.* **2019**, *58*, 15841–15847. [[CrossRef](#)] [[PubMed](#)]
98. Cao, L.; Li, D.; Hu, E.; Xu, J.; Deng, T.; Ma, L.; Wang, Y.; Yang, X.Q.; Wang, C. Solvation structure design for aqueous Zn metal batteries. *J. Am. Chem. Soc.* **2020**, *142*, 21404–21409. [[CrossRef](#)]
99. Xu, Z.; Li, H.; Liu, Y.; Wang, K.; Wang, H.; Ge, M.; Xie, J.; Li, J.; Wen, Z.; Pan, H.; et al. Durable modulation of Zn(002) plane deposition via reproducible zincophilic carbon quantum dots towards low N/P ratio zinc-ion batteries. *Mater. Horiz.* **2023**, *10*, 3680–3693. [[CrossRef](#)]
100. Chen, R.; Zhang, W.; Huang, Q.; Guan, C.; Zong, W.; Dai, Y.; Du, Z.; Zhang, Z.; Li, J.; Guo, F.; et al. Trace Amounts of Triple-Functional Additives Enable Reversible Aqueous Zinc-Ion Batteries from a Comprehensive Perspective. *Nano-Micro Lett.* **2023**, *15*, 81. [[CrossRef](#)]
101. Wang, S.B.; Ran, Q.; Yao, R.Q.; Shi, H.; Wen, Z.; Zhao, M.; Lang, X.Y.; Jiang, Q. Lamella-nanostructured eutectic zinc-aluminum alloys as reversible and dendrite-free anodes for aqueous rechargeable batteries. *Nat. Commun.* **2020**, *11*, 1634. [[CrossRef](#)]
102. Liang, Y.; Ding, W.; Yao, B.; Zheng, F.; Smirnova, A.; Gu, Z. Mediating Lithium Plating/Stripping by Constructing 3D Au@Cu Pentagonal Pyramid Array. *Batteries* **2023**, *9*, 279. [[CrossRef](#)]
103. Su, S.; Xu, Y.; Wang, Y.; Wang, X.; Shi, L.; Wu, D.; Zou, P.; Nairan, A.; Lin, Z.; Kang, F.; et al. Holey nickel nanotube reticular network scaffold for high-performance flexible rechargeable Zn/MnO<sub>2</sub> batteries. *Chem. Eng. J.* **2019**, *370*, 330–336. [[CrossRef](#)]
104. Kang, Z.; Wu, C.L.; Dong, L.B.; Liu, W.B.; Mou, J.; Zhang, J.W.; Chang, Z.W.; Jiang, B.Z.; Wang, G.X.; Kang, F.Y.; et al. 3D porous copper skeleton supported zinc anode toward high capacity and long cycle life zinc ion batteries. *Acs Sustain. Chem. Eng.* **2019**, *7*, 3364–3371. [[CrossRef](#)]

105. Qiu, W.; Li, Y.; You, A.; Zhang, Z.; Li, G.; Lu, X.; Tong, Y. High-performance flexible quasi-solid-state Zn–MnO<sub>2</sub> battery based on MnO<sub>2</sub> nanorod arrays coated 3D porous nitrogen-doped carbon cloth. *J. Mater. Chem. A* **2017**, *5*, 14838–14846. [[CrossRef](#)]
106. Li, M.; Meng, J.; Li, Q.; Huang, M.; Liu, X.; Owusu, K.A.; Liu, Z.; Mai, L. Finely crafted 3D electrodes for dendrite-free and high-performance flexible fiber-shaped Zn-Co batteries. *Adv. Funct. Mater.* **2018**, *28*, 1802016. [[CrossRef](#)]
107. Wang, X.; Wang, F.; Wang, L.; Li, M.; Wang, Y.; Chen, B.; Zhu, Y.; Fu, L.; Zha, L.; Zhang, L.; et al. An aqueous rechargeable Zn/Co<sub>3</sub>O<sub>4</sub> battery with high energy density and good cycling behavior. *Adv. Mater.* **2016**, *28*, 4904–4911. [[CrossRef](#)]
108. Zeng, Y.; Zhang, X.; Qin, R.; Liu, X.; Fang, P.; Zheng, D.; Tong, Y.; Lu, X. Dendrite-free zinc deposition induced by multifunctional CNT frameworks for stable flexible Zn-ion batteries. *Adv. Mater.* **2019**, *31*, e1903675. [[CrossRef](#)]
109. Tian, Y.; An, Y.; Wei, C.; Xi, B.; Xiong, S.; Feng, J.; Qian, Y. Flexible and free-standing Ti<sub>3</sub>C<sub>2</sub>TxMXene@Zn paper for dendrite-free aqueous zinc metal batteries and nonaqueous lithium metal batteries. *ACS Nano* **2019**, *13*, 11676–11685. [[CrossRef](#)]
110. Liu, C.; Luo, Z.; Deng, W.; Wei, W.; Chen, L.; Pan, A.; Ma, J.; Wang, C.; Zhu, L.; Xie, L.; et al. Liquid alloy interlayer for aqueous zinc-ion battery. *ACS Energy Lett.* **2021**, *6*, 675–683. [[CrossRef](#)]
111. Wang, L.; Huang, W.; Guo, W.; Guo, Z.H.; Chang, C.; Gao, L.; Pu, X. Sn alloying to inhibit hydrogen evolution of Zn metal anode in rechargeable aqueous batteries. *Adv. Funct. Mater.* **2021**, *32*, 2108533. [[CrossRef](#)]
112. Qi, Z.; Xiong, T.; Chen, T.; Yu, C.; Zhang, M.; Yang, Y.; Deng, Z.; Xiao, H.; Lee, W.S.V.; Xue, J. Dendrite-free anodes enabled by a composite of a ZnAl alloy with a copper mesh for high-performing aqueous zinc-ion batteries. *ACS Appl. Mater. Interfaces* **2021**, *13*, 28129–28139. [[CrossRef](#)] [[PubMed](#)]
113. Cao, P.; Zhou, X.; Wei, A.; Meng, Q.; Ye, H.; Liu, W.; Tang, J.; Yang, J. Fast-charging and ultrahigh-capacity zinc metal anode for high-performance aqueous zinc-ion batteries. *Adv. Funct. Mater.* **2021**, *31*, 2100398. [[CrossRef](#)]

**Disclaimer/Publisher’s Note:** The statements, opinions and data contained in all publications are solely those of the individual author(s) and contributor(s) and not of MDPI and/or the editor(s). MDPI and/or the editor(s) disclaim responsibility for any injury to people or property resulting from any ideas, methods, instructions or products referred to in the content.